Hybrid Model for Bulk Current Injection Probe

Issa M. Mashriki, S.M.J. Razavi, S.H.M. Armaki
Faculty of Electrical & Computer Engineering, Malek Ashter University of Technology, Iran.
Issa_mashriki@mut.ac.ir, razavismj@mut.ac.ir, mohseni@mut.ac.ir
Corresponding Author: razavismj@mut.ac.ir

***Abstract*- A new hybrid-model for BCI probe is derived. This model is built based on the probe's internal structure without refinements, and by carrying out just one electrical measurement for the reflection coefficient, so that it can be generalized and used in studying the effect of layout parameters in the aim of improving the probe high frequency performance, which helps the developer in design stage. The hybrid-model is validated versus extracted permeability spectra, voltage transfer ratio and series impedance for the probe F-130A. The comparison is made between the derived hybrid-model and that of explicit model, the results show good accordance between them. An application for the model is illustrated to bring to light its effectiveness.**

***Index Terms*-** Bulk current injection (BCI), complex permeability spectra, electromagnetic Compatibility (EMC), modeling, transmission line (TL).

I. INTRODUCTION

Bulk current injection probe (BCI) is a conducted-susceptibility (CS) test device based on the injection of common-mode (CM) noise currents in bundles of wires and cables. It is widely used in electromagnetic compatibility (EMC) test procedures. BCI-based techniques have progressively gained the attention of several international standards, because they permit interference testing at the early design stage without making any change in the device connections, and provide a low-cost way to verify the immunity against radiated interference when compared with the classical test procedures in fully-anechoic chamber (FAC). These advantages made BCI techniques accepted by all regulatory standards [1]-[6].

Recently, many efforts were done in modeling and characterizing the BCI probes. Some activities are based on measuring S-parameters or lumped elements parameters [7]-[11] which differ from probe to another. Further attempts use the circuit concept approach which replaces the probe with its equivalent source voltage and current without taking into account its main characteristics as in [12]-[14]. Some models utilize software optimization or refinements in evaluating the model needed

Manuscript received 3-Oct.-2019 and revised 28-Nov.-2019, *P- ISSN: 2322-4088*
Accepted on 17- Dec.-2019 *E- ISSN: 2322-3936*

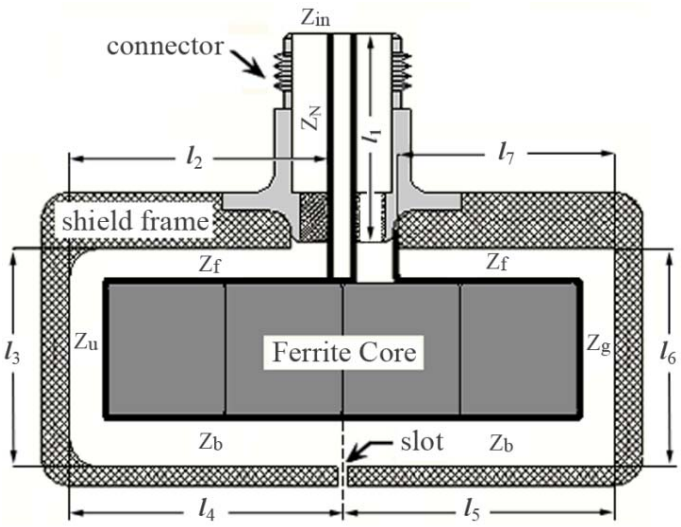

Fig. 1. Radial cross-section of a general type BCI probe with its input connector and layout parameters.

parameters as in [15] and [16]. Other works carry out 2D and 3D electromagnetic models as in [17]-[19], in which the complex permeability spectra is the main parameter that must be known.

Even if some models give an excellent results which nearly coincide with measurements like the explicit model [9], but it can't be used in design stage, because of the refinements included in it. For example, the transmission line formed between the primary winding and the probe frame was represented by the refined lumped elements C_{w1} and L_{w1} for the probe F-130A, which prevent using it in modeling other versions of BCI-probes without knowing its corresponding refined parameters.

Therefore, it is important to search on a more practical circuit model so that it can be used in design stage, which means to simulate the real dimensions without achieving any refinement. As would be shown, the probe is designed so carefully, and each dimensional parameter has its own effect on the probe performance, all the derived models doesn't carefully clarify the role of this parameters on the probe performance, which make it useless while designing a new probe with a special features.

In this paper, TL theory would be used in modeling the probe F-130A with its connector. The rules used in modeling the proposed probe are general, and can be used in modeling any BCI probe of the same internal structure, and can be altered to match other structures. This paper includes also to extract the ferrite core complex permeability spectra, and to provide a method for extracting the voltage transfer ratio and series impedance. This work can be considered as a development to the hard work achieved in [9], which has been used in many later articles [16], [20] and [21].

II. INJECTION PROBE CHARACTERIZATION

The BCI probe is a wide band power transformer, with mostly single turn primary coil wound around a toroidal ferrite core. Fig. 1 illustrates a radial cross sectional view of a typical BCI probe, the

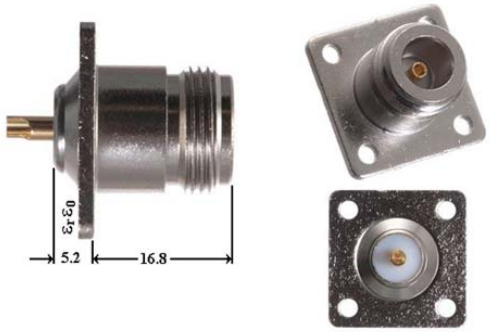

Fig. 2. N Female Solder Chassis Mount Connector-RG58.

terminals of primary coil are connected to a N-type 50Ω RF-connector, one terminal is attached to the inner pin while the other one is connected to the external shield. The probe is shielded using two identical aluminum frames connected together with the outer shield of the connector from the outer side of the probe, and separated by a small slot from the inner one.

Typically [22], all injection probes are equipped with the Type-N connector shown in Fig. 2, which has a detailed trade description as "N Female Solder Chassis Mount Connector-RG58". This connector has a maximum operating frequency of 11GHz which is much higher than any BCI probe working range of frequencies. It has a characteristic impedance of 50Ω, and a total length of about l_1=22mm. Thus, the connector can be modeled with a TL of length l_1 insulated with Teflon (PTFE) with dielectric constant of 2.1.

III. HYBRID-MODEL DERIVATION AND INTERPRETATION

The cross sectional view of Fig. 1, shows that the space between the primary coil and the shield frame varies along the coil circumference, this changes the characteristic impedance from section to another, the proposed hybrid-model in Fig. 3(a) takes this changes into account. The characteristic impedance of each section is represented in its order. The model expresses the probe when clamped onto the conductor under test, in which the mutual inductance M denotes the coupling between the probe's inductor L_1 and the conductor under test L_2, with L_1=M and L_2=M+L_{2d}, where L_{2d} denotes the leakage inductance. Using the T-equivalent model of two coupled inductors, the hybrid-model can be altered to be as shown in Fig. 3(b).

When clamped onto a conductor under test, the BCI probe can be replaced by its equivalent voltage source V_S in connection with a series impedance Z_P. These quantities can be extracted from measures scattering parameters with the help of the implicit model developed in [9]. While V_S is in proportion to the RF voltage source V_{RF}, the series impedance relates to the leakage inductance L_{2d} which changes according to the test setup.

In the model, the connector is considered between port 0 and port 1. The characteristic impedances

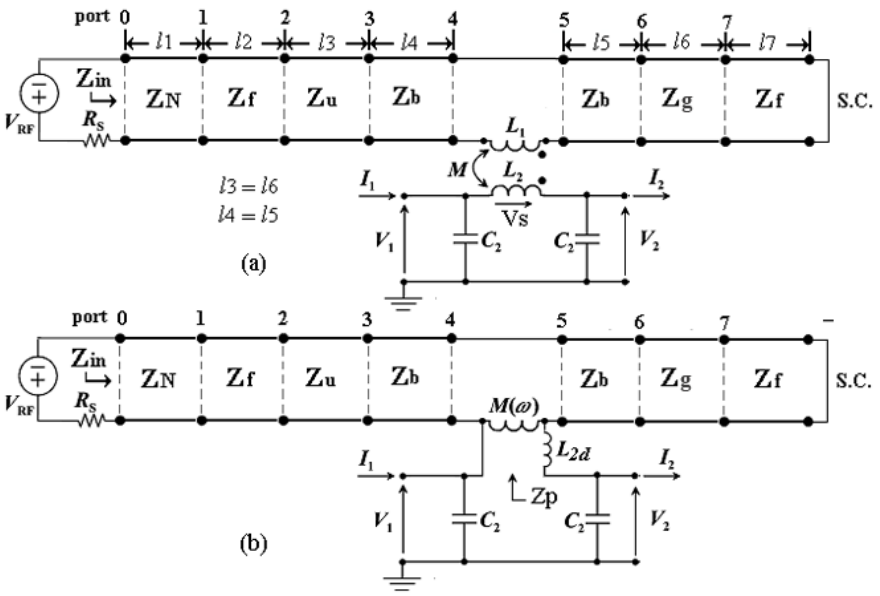

Fig. 3. (a) Hybrid-model of the injection probe clamped onto the conductor under test, and (b) its T-equivalent model.

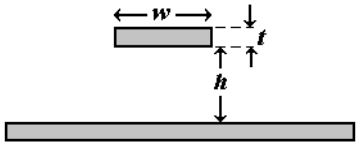

Fig. 4. Microstrip parameters.

Z_f, Z_u, Z_b and Z_g are calculated using microstrip line formula (1) [23-Ch4], with the parameters defined in Fig. 4, assuming the land thickness is zero (t=0), and the space between the primary coil and shield frame is filled homogeneously with air, as insulating medium.

$$Z = 120\pi \left[\frac{w}{h} + 1.393 + 0.667 \times ln\left(\frac{w}{h} + 1.444\right)\right]^{-1} \quad (1)$$

Where *w* denotes the width of the probe's primary single turn.

IV. EXTRACTING THE MODEL EQUIVALENT PARAMETERS

A. Extracting the Complex Permeability

The complex permeability can be extracted apart from measured input reflection coefficient or input impedance in the absence of secondary circuit. Formula (2) is used to calculate the probe input impedance Z_{in} apart from measured reflection coefficient S_{11}, then the impedance Z_4 at port 4 as seen from the load side, and the impedance Z_5 at port 5 as seen from the source side can be calculated strictly using TL impedance formula.

$$Z_{in}(\omega) = 50\frac{1+S_{11}}{1-S_{11}} \quad (2)$$

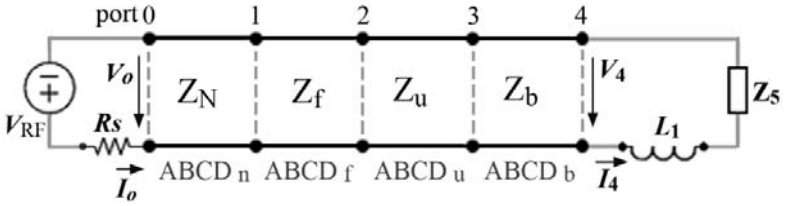

Fig. 5. Defining matrix parameters used in calculating Vs.

Z_5-Z_4 represents the impedance of the primary coil ($j\omega L_1$). After extracting L_1, the complex permeability can be retrieved using (3)

$$\hat{L}_1(\omega) = \mathrm{L}_0(\hat{\mu}_r'(\omega) - j\hat{\mu}_r''(\omega)) \tag{3}$$

Where L_0 denotes the inductance that would be measured if the core had unity permeability, under the condition that flux distribution remains unaltered. According to [9], L_0 can be estimated using the following coaxial cable inductance relation.

$$L_0 = \frac{\mu_o b}{2\pi} \ln\left(\frac{r'_{out}}{r'_{in}}\right) \tag{4}$$

where b, r'_{out}, and r'_{in} denote the height, the outer radius, and the inner radius of the ferrite toroidal core, respectively.

B. Extracting the Transfer Ratio

The probe's output voltage Vs is calculated as

$$V_S = sMI_4 \tag{5}$$

In which I_4 denotes the current passing out of port 4, as shown in Fig. 5, and M=L_1 as calculated in the previous section. I_4 is calculated using the general ABCD matrix of short TL (6).

$$ABCD_m \approx \begin{bmatrix} 1 & jZ_m B_m l_m \\ jB_m l_m / Z_m & 1 \end{bmatrix} \tag{6}$$

Where l_m, B_m and Z_m are the length, propagation constant and characteristic impedance of considered TL. Firstly, the ABCD matrix between port 0 and port 4 is calculated using (7), and since V_0 relates to I_0 by (8) and V_4 relates to I_4 by (9), this gives the expression in (10) for I_4.

$$\begin{bmatrix} V_4 \\ I_4 \end{bmatrix} = \left(ABCD_n ABCD_f ABCD_u ABCD_b\right)^{-1} \begin{bmatrix} V_0 \\ I_0 \end{bmatrix} = \begin{bmatrix} A & B \\ C & D \end{bmatrix} \begin{bmatrix} V_0 \\ I_0 \end{bmatrix} \tag{7}$$

$$\mathrm{V}_0 = \mathrm{V}_{\mathrm{RF}} - \mathrm{R}_\mathrm{s}\mathrm{I}_0 \tag{8}$$

$$V_4 = (Z_{L1} + Z_5)I_4 \tag{9}$$

$$I_4 = \frac{\Delta \cdot V_{RF}}{R_S A - B - (sL_1 + Z_5)(R_S C - D)} \tag{10}$$

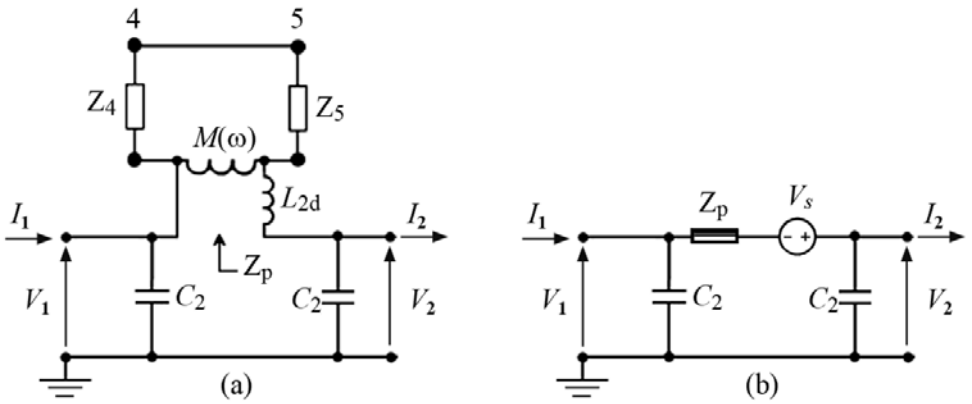

Fig. 6. (a) The equivalent model used in calculating Z_P.(b) The probe is replaced by its equivalent source *Vs* and series impedance Zp.

in which Δ denotes the determenant of the ABCD matrix defined in (7), and s=jω denotes Laplace coefficient. The voltage transfer ratio is defined by the quantity Vs/V_{RF} and is calculated directly by placing (10) in (5).

C. Extracting the Equivalent Series Impedance

To extract the equivalent series impedance Z_P, the coupling between L_1 and L_2, is first replaced by its equivalent T-model, which in final form gives the circuit shown in Fig. 6(a). Z_4 is calculated without considering the RF source, and as shown from the load. Z_P is the sum of sL_{2d} and the connection in parallel of sM, and Z_4+Z_5, thus it has the following expression

$$Z_p = sL_{2d} + \frac{sM(Z_4+Z_5)}{sM+(Z_4+Z_5)(1+s^2MC_d)} \tag{11}$$

The leakage inductance L_{2d}, which is considered in the secondary inductance is representative for probe to clamped wire interactions, thus, its values depend on the characteristics of the clamped conductor or the actual test setup. It can be approximated by the total inductance of an imaginary coaxial TL whose cross section extends from the clamped wire to the inner surface of the shield and is estimated as

$$L_{2d} \approx \frac{\mu_0}{2\pi} \ln\left(\frac{r_{in}}{r_w}\right) \cdot l_{probe} \tag{12}$$

Where r_w , l_{probe} denote the radius of the clamped conductor and the probe length, respectively.

After extracting *Vs* and *Zp*, the model can be simplified to become as shown in Fig. 6(b), in [9], it was referred to this model as the implicit model, in which a procedure was developed for extracting *Vs* and *Zp* from measurement data. This allows validating any developed model for the probe versus *Vs* and *Zp*.

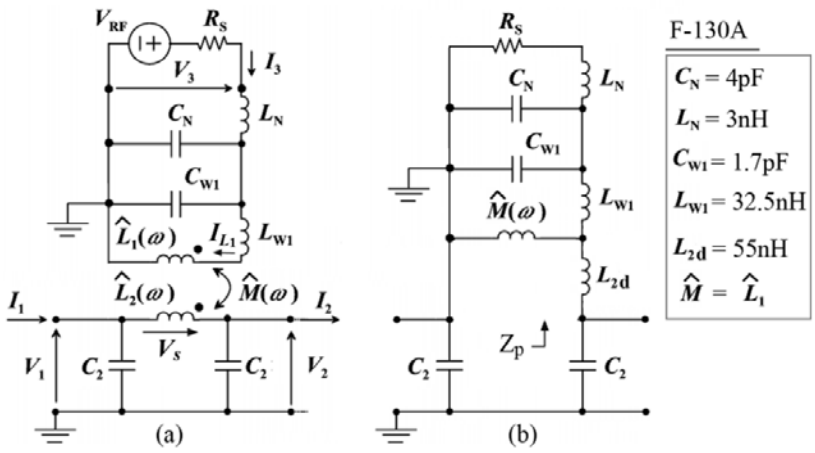

Fig. 7. (a) Explicit model [9] and (b) its T-equivalent model used for extracting the series impedance Zp, with the model parameters used for the probe model F-130A.

V. VERIFYING THE HYBRID-MODEL

Verifying the model implies to verify its extracted complex permeability μ_r, voltage transfer ratio V_S/V_{RF} and series impedance Z_P spectra for an injection probe. Measuring the permeability spectra requires to take a sample of the probe's core to be measured using microwave procedures, which leads to take the probe into useless pieces and this is not at the user disposal. Another way is to compare the permeability spectra with that extracted using a previously validated model, therefore, the explicit-model developed in [9] would be used.

A. Overview

The explicit model is shown in Fig. 7(a), in which (C_N, L_N) and (C_{w1}, L_{w1}) are the lumped element representation for the input connector and the transmission line formed between the primary winding and the shield, respectively. The probe's equivalent source *Vs* can be extracted directly from this model, while Fig. 7(b) is used to extract its equivalent series impedance. The formulas expressing these parameters are:

$$V_S = sMI_{L1} = \frac{sM \cdot V_{RF}}{s(L_1+L_{w1})+(R_S+sL_N)(1+s^2(C_N+C_{w1})(L_1+L_{w1}))} \tag{12}$$

$$Z_p = sL_{2d} + \frac{sMZ}{sM+Z} \tag{13}$$

$$Z = sL_{w1} + \frac{sL_N+R_s}{1+s(C_N+C_{w1})(sL_N+R_s)} \tag{14}$$

Where Z denotes the total primary impedance as seen from the primary coil.

Table I. F-130A dimensional (in mm) and electrical parameters

l_2	$l_3 = l_6$	$l_4 = l_5$	l_7	W	h_f	h_u	h_b
27.5	23	29	23	10	2	3.5	5
Z_N	Z_f	$Z_u = Z_g$	Z_b				
50Ω	49.37 Ω	72.18 Ω	89.38 Ω				

This model was validated by comparing the precedent parameters with that extracted from the implicit model for the probe model F-130A, with the values shown in Fig. 7. Repeating the long procedure of implicit model for validating the hybrid-model would increases the size of this paper without adding a novelty. Therefore, it is sufficient to compare the results of hybrid-model with that of explicit model for the BCI probe type F-130A used in it.

B. F-130A Characterization

The model parameters for the probe F-130A are listed in Table. I, the first raw represents the dimensions retrieved from the probe layout, while the second row represents calculated impedances using formula (1). The maximum frequency of interest for the most BCI probes is lower than 1GHz (de facto 450MHz for the proposed one), which gives a minimum wavelength of λ_{min} =30cm, thus, all defined TLs has a length of less than $0.1\lambda_{min}$, and can be considered as electrically short TLs. Table I discloses that the probe was designed to start with a matched TL (Z_f), then continues with step-up characteristic impedances, then is followed by a step-down characteristic impedances, and ends with a short circuit. This is a good starting point when designing a new BCI-probe, which can't be concluded from the explicit model.

The other needed parameters are:

r_{in}=16mm, l_{probe}=64mm, r'_{in}=24mm, r'_{out}=39mm, b=50mm and r_w=0.4mm,

Which gives L_0=4.855nH and L_{2d}=47.2nH.

C. Verification versus Complex permeability

We need first to measure the probe's reflection coefficient, but in [24], Fig. 2 shows that two F-130A type probes with different serial numbers have a little different characteristics, especially at medium and low frequencies, therefore, the comparison would not complete and give the correct impression unless it done on the same F-130A type probe and with the same measuring tools.

From this point we are forced to use the input impedance of the F-130A probe used in [9]. The proposed probe input impedance or reflection coefficient in case of eliminating the secondary circuit are not reported in [9]. Although, measuring the input impedance is less hard than gathering data to retrieve the probe input impedance using the explicit model, but the strict comparison enforce us to go on in this work. The work is done by filling the complex permeability extracted from the explicit

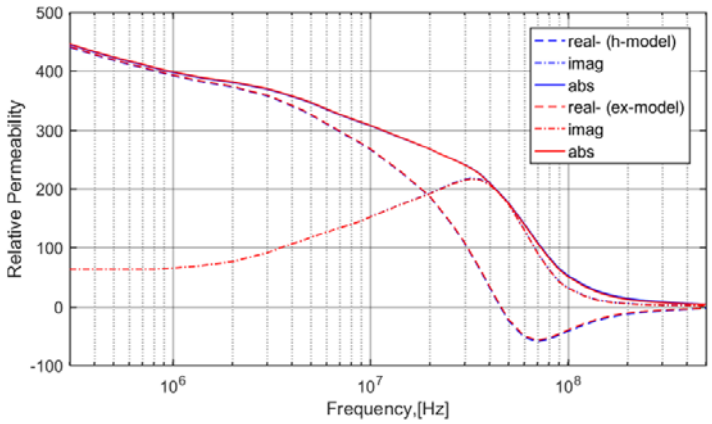

Fig. 8. The complex permeability spectra of the ferrite core of the injection probe F-130A as extracted from hybrid-model and explicit model.

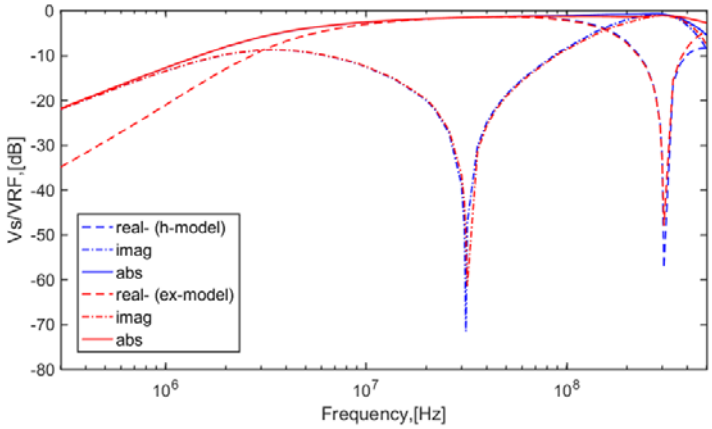

Fig. 9. The voltage transfer ratio spectra of the injection probe F-130A as extracted from hybrid-model and explicit model.

model derived in ([9], Fig. 12) into two MATLAB vectors one for the real part and the second for the imaginary part. This would help in retrieving the input impedance of used probe using the explicit-model, and later in comparing the complex permeability spectra extracted from hybrid-model with that extracted from explicit model.

Retrieving the probe input impedance from the permeability spectra is done apart from the explicit model of Fig. 7(a) after omitting the secondary winding, which leads to the expression (15) for Zin, with considering formula (3) for L_1.

$$Z_{in} = sL_N + \frac{s(L_1+L_{W1})}{1+s^2(C_N+C_{W1})(L_1+L_{W1})} \tag{15}$$

A MATLAB code program is achieved to do the so called procedure. The plot in Fig. 8 compares the permeability spectra resulted from the hybrid-model as proposed in section IV-A with that resulted from the explicit model. The result shows a good agreement between them.

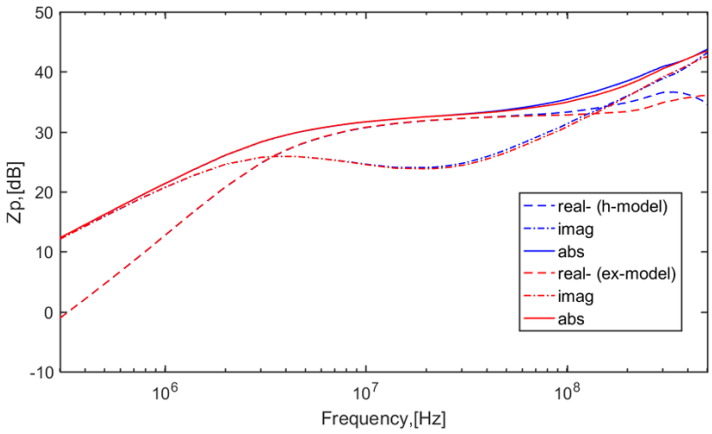

Fig. 10. The series impedance spectra of the injection probe F-130A as extracted from hybrid-model and explicit model.

D. Verification Versus Voltage Transfer Ratio

A MATLAB code program was achieved for calculating and plotting the voltage transfer ratio of the hybrid-model as proposed in IV-B and to compare it with that from the explicit for the probe F-130A. The plot shown in Fig. 9 illustrates that the voltage transfer ratio of hybrid-model is in good agreement with that extracted from the explicit model. While a comparison between the explicit-model and measurements achieved using the implicit-model was reported in ([9]- Fig. 9)

E. Verification Versus the Series Impedance

A MATLAB program is achieved to extract and plot the equivalent series impedance of hybrid-model as proposed in IV-C, and to compare it with that extracted from the explicit-model for the probe F-130A. The plot shown in Fig. 10 shows that the equivalent series impedance of hybrid-model is in good agreement with that extracted from explicit model at low and medium frequencies, while a little increase in estimated phase and amplitude appears at high frequencies. A comparison between the explicit-model and measurements achieved using the implicit-model was reported in ([9]- Fig. 10).

VI. ANALYSIS AND INTERPRETATION

The previous verifications prove the correctness of the procedures, formulas and assumptions made in deriving the hybrid-model. The microstrip formula (1) is used in calculating the TL impedances without considering the ferrite existence and the results prove the correctness of this assumption, which means that the ferrite must not be taken into account in calculating the model parameters except for L_1. It maybe thought that the effect of ferrite must be introduced in calculated TL impedances, because the TL is represented by distributed L-C equivalent circuit. Therefore, in addition to the precedent proof, we need to interpret this point in detail.

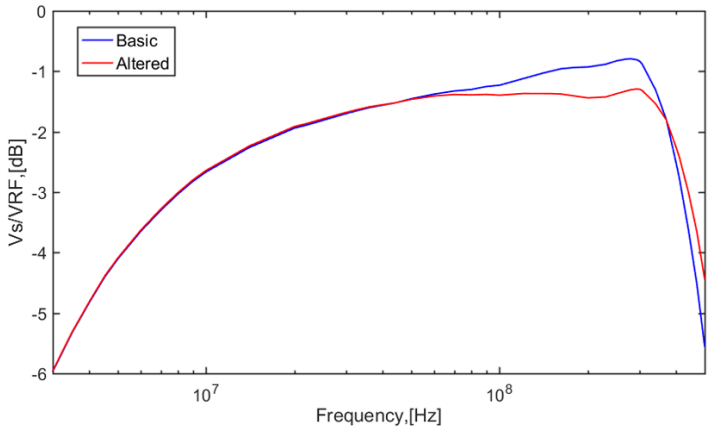

Fig. 11. Effect of achieving the proposed changes in the shield on predicted magnitude of transfer ratio.

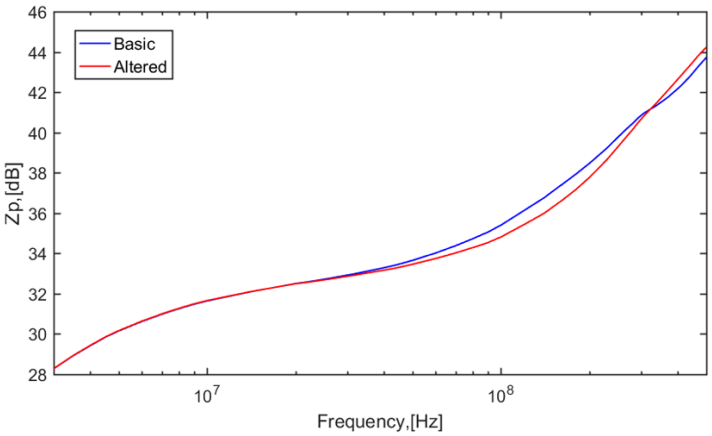

Fig. 12. Effect of achieving the proposed changes in the shield on predicted magnitude of series impedance.

As far as we know, from switched mode power supplies basic principles, when a ferrite core is wound with a coil of many turns, the winding capacitance is represented in parallel with the coil inductance, and is calculated solely without considering the ferrite because this is a case of superposition, which means that, in modeling, each element is considered alone without considering the effect of other parameters, and connecting these elements correctly together in the circuit model has the responsibility to show this effect, otherwise, each effect would be shown twice in the model, and thus, the model could not be validated. Even if it was not strictly declared, there are many examples and articles apply this idea, as in antennas, optics and TL theory.

VII. APPLICATION

The model is used to see the effect of altering the shield, therefore, the separating distance between the shield and core is made equals to 2 mm from all sides, this leads to an equal characteristic impedance of 50Ω in all TL sections of the model. The result of achieving this change on the magnitude of transfer ratio and series impedance is shown in Figs. 11 and 12, respectively.

Predicted results from hybrid-model shows that, the proposed change affects the high frequency response of the probe by decreasing the transfer ratio and equivalent series impedance below about 350MHz, and increases it above this frequency, this improves a little the probe working band of frequencies on the base of degrading the probe characteristics at medium frequencies.

VIII. CONCLUSION

A new hybrid-model for BCI probe is derived, procedures for extracting the relative permeability, transfer ratio and series impedance spectra are proposed and validated by comparing it with that extracted from the explicit model. It was shown that the ferrite does not need to be taken into consideration wile calculating the model parameters except for the probe's primary inductance. The model is derived based on the probe configuration using TL theory without optimizations or refinements in estimating its parameters, therefore, it is characterized by two advantages: First, it can be used in modeling any BCI probe with the same internal structure, and can be altered to match other versions. Second, it can be used in studying the effect of the probe's layout parameters on its performance. An example application was presented, in which the shield is altered to see its effect. The achieved change showed a little improve in the probe working band of frequency with lowering the probe characteristics at medium frequencies below 350MHz.

REFERENCES

[1] RTCA/DO-160F, Environmental conditions and test procedures for airborne equipment, 2007.

[2] Electromagnetic compatibility (EMC) -Part4–6: Testing and measurement techniques— Immunity to conducted disturbances, induced by radio-frequency fields, IEC Standard 61000-4-6, May 2006.

[3] ISO Standard 11451-4: Road vehicles-Vehicle test methods for electrical disturbances from narrowband radiated electromagnetic energy-Part4: Bulk Current Injection (BCI), June, 2006.

[4] ISO Standard 11452-4: Road Vehicles- Component Test Methods for Electrical Disturbances From Narrowband Radiated Electromagnetic Energy-Part4: Harness excitation methods, Dec.2011.

[5] IEC 62132-3, Ed.1: Integrated Circuit Measurements of Electromagnetic Immunity 150kHz to 1GHz, Part 3: Bulk Current Injection (BCI) Method, 2007.

[6] Department of Defense Interface Standard, Requirements for the Control of Electromagnetic Interference Characteristics of Subsystems and Equipment, *MIL-STD-461E*, Aug. 20, 1999.

[7] G. Cerri, R. DeLeoe, V. Mariani Primiani, S. Pennesi, and P. Russo, “Wide-band characterization of current probes,” *IEEE Trans. Electromagn. Compat*., vol. 45, no. 4, pp. 616–625, Nov. 2003.

[8] F. Grassi, S.A. Pignari, and F. Marliani, “Improved lumped-Pi circuit model for bulk current injection probes,” *Proc. IEEE Symp. Electromagn. Compat*., Chicago, IL, 8-12 Aug. 2005, pp.451–456.

[9] F. Grassi, F. Marliani, and S.A. Pignari, "Circuit Modeling of Injection Probes For Bulk Current Injection," *IEEE Trans. Electromagnetic. Compatibility*., vol. 49, no. 3,pp. 563-576, Aug. 2007.

[10] B. P. Nayak, A. Das, S. R. Vedicherla, and D. Gope, "Circuit Models for Bulk Current Injection (BCI) Clamps with Multiple Cables," *IEEE Intern. Symp. on Electromagnetic Compatibility (EMC),* May. 2018.

[11] W. Zhao, Z. Yan, and W. Liu, "Two methods for BCI probe to improve the high frequency performance,” *, 11th IEEE Intern. Symp. on Antennas, Propagation and EM Theory (ISAPE)*, Oct. 2016.

[12] K. Murano, N. Takata, M. Tayarani, F. Xiao, and Y. Kami, "Analysis of Transmission Line Loaded with BCI Probe using Circuit Concept Approach", *IEICE Communications Express*, vol. 4, no. 7, pp. 223-227, 2015.

[13] K. Murano, N. Takata, M. Tayarani, "Theoretical Analysis of BCI Test System using Circuit Concept Approach," *IEEE Intern. Symp. on Electromagnetic Compatibility (EMC),* July. 2016.

[14] K. Murano, M. Hoshino, M. Tayarani, F. Xiao, Y. Kami, "Modeling of Transmission Line Loaded with BCI Probe Using Circuit Concept Approach", *IEEE Intern. Symp. on Electromagnetic Compatibility (EMC),* Sep. 2017.

[15] F. Lafon, Y. Belakhouy, and F. De Daran "Injection probe modeling for bulk current injection test on multi conductor transmission lines," *IEEE Symp. on Embedded EMC Proceedings*, Rouen, France, Oct. 18-19, 2007.

[16] F. Grassi, F. Marliani, and S.A. Pignari, "SPICE modeling of BCI probes accounting for the frequency-dependent behavior of the ferrite core," *Proc. XIXth General Assembly of International Union of Radio Science* (U. R.S. I), Chicago, IL, USA, pp. 7-16, Aug. 2008.

[17] M.S. Diop, E. Clavel, H. Cheaito, C. Vollaire, and E. Vialardi, "2D modeling of Bulk Current Injection Probe and Validation with Measurements," *32nd General Assembly and Scientific Symposium of the International Union of Radio Science* (URSI GASS), Montreal, 19-26 Aug. 2017.

[18] P. DeRoy, S. Piper, "Full-wave Modeling of Bulk Current Injection Probe Coupling to Multi-conductor Cable Bundles," *IEEE Inter. Symp. on Electromag. Compatib*., July 2016.

[19] N. Toscani, F. Grassi, G. Spadacini, and S. A. Pignari, "Circuit and Electromagnetic Modeling of Bulk Current Injection Test Setups Involving Complex Wiring Harnesses," *IEEE Trans. Electromagnetic. Compatibility,* vol. 60, no. 6, pp. 1752-1760, Dec. 2018.

[20] F. Grassi, "Accurate Modeling of Ferrite-Core Effects in Probes for Bulk Current Injection," *Proc. 2009 IEEE Int. Conf. on Microw., Commun., Antenna and Elec. Systems*, IEEE COMCAS, Nov. 2009, pp.1-6.

[21] F.Grassi, S.A.Pignari, and G.Spadacini, "Time-Domain Response of Bulk Current Injection Probes to Impulsive Stress Waveforms," *IEEE Inter. Symposium on Electromagnetic Compatibility,* Dresden, Germany, Aug. 2015.

[22] Fischer Custom Communications BCI Brochure, Fischer Custom Communications, Inc.

[23] C.R.Paul, Introduction to Electromagnetic Compatibility, 2nd Ed. NewYork: Wiley–Interscience,2006

[24] F.Grassi, G.Spadacini, F.Marliani, and S.A.Pignari "Use of Double Bulk Current Injection for Susceptibility Testing of Avionics," *IEEE. Trans. Electromag. Comp.,* vol. 50, no. 3, pp. 524-535, Aug 2008.